

# The impact range for smooth wall-liquid interactions in nanoconfined liquids

Trond S. Ingebrigtsen<sup>1,\*</sup> and Jeppe C. Dyre<sup>1</sup>

<sup>1</sup>*DNRF Centre “Glass and Time”, IMFUFA, Department of Sciences,  
Roskilde University, Postbox 260, DK-4000 Roskilde, Denmark*

(Dated: January 2, 2022)

Bulk and nanoconfined liquids have initially very different physics; for instance, nanoconfined liquids show stratification and position-dependent relaxation processes. A number of similarities between bulk and nanoconfined liquids have nevertheless been reported in computer simulations during the last decade. Inspired by these observations, we present results from molecular dynamics computer simulations of three nanoconfined liquids (i.e., single-component Lennard-Jones (LJ) liquid, Kob-Andersen binary LJ mixture, and an asymmetric dumbbell model) demonstrating also a microscopic similarity between bulk and nanoconfined liquids. The results show that the interaction range for the wall-liquid and liquid-liquid interactions of the nanoconfined liquid are identical to the bulk liquid as long as the liquid remains “Roskilde simple” in nanoconfinement, i.e., the liquid has strong correlations between virial and potential energy equilibrium fluctuations in the  $NVT$  ensemble.

## I. INTRODUCTION

Bulk and nanoconfined liquids have apparently very different physics. The confining boundaries not only bias the average spatial distribution of the constituent molecules, but also the ways by which those molecules can dynamically rearrange. These effects have been exploited in the design of coating, nanopatterning, and nanomanufacturing technologies<sup>1,2</sup>. They have also been experimentally characterized for a wide variety of material systems, including small-molecule fluids<sup>3–10</sup>, polymers<sup>11–16</sup>, ionic liquids<sup>17</sup>, liquid crystals<sup>18</sup>, and dense colloidal suspensions<sup>19–23</sup>, as well as studied extensively via computer simulations<sup>22,24–31</sup>.

A number of similarities between bulk and nanoconfined liquids have nevertheless been observed during the last decade. For example, it has been discovered that Rosenfeld’s excess entropy scaling<sup>32</sup> – in which a dimensionless transport coefficient is correlated with the excess entropy (with respect to an ideal gas) – is unaffected by the spatial confinement<sup>33–36</sup>. This also turns out to be valid for excess isochoric heat capacity scaling<sup>36</sup> and for Rosenfeld-Tarazona’s expression for the specific heat<sup>37,38</sup>. Similarly, it has been shown that the continuum Navier-Stokes equations extend into the nanoscale regime by the inclusion of coupling between linear and angular momentum<sup>39–42</sup>. Likewise have attempts at extending bulk mode-coupling theory<sup>43</sup> to the nanoscale been fruitful<sup>44–46</sup>. These results are naturally very intriguing since they indicate that fundamentally new theories may not be needed to describe the physics of the nanoscale. At the same time, the results are also quite puzzling given the fact that bulk and nanoconfined liquids have very different phenomenology.

In this connection, it is thus natural to wonder whether these similarities extend to a more fundamental or “mi-

croscopic” level. In fact, the mere difference between bulk and nanoconfined liquids is the external potential constituting the spatial confinement. The study of confinement is nevertheless complicated by the fact that the confining boundaries (the “walls”) do not only impose a geometrical constraint on the liquid, but also energetic costs. Several investigations have tried to separate the entropic and energetic contributions to the physics by studying, e.g., hard-sphere walls<sup>47</sup>, reflecting walls<sup>48</sup>, amorphous walls<sup>26,49</sup>, and more. With the above mentioned similarities in mind, a “microscopic” conjecture motivated from these studies is that the interaction range for the wall-liquid and liquid-liquid interactions of the nanoconfined liquid is identical to that of the bulk liquid.

The relevant range of interaction for bulk liquids was considered long ago by traditional liquid-state theories<sup>50,51</sup> and is captured in the well-known Weeks-Chandler-Andersen (WCA) approximation<sup>51</sup> in which the pair potential is truncated at the potential minimum. In this picture, the attractive pair forces of typical liquid-state configurations cancel to a good approximation and only contribute with a negative background potential<sup>50</sup>. The relevance of a sharp distinction between repulsive and attractive pair forces of the bulk liquid has, however, recently been questioned<sup>52–54</sup>. Instead, it has been suggested that the relevant distinction is between the forces within the first coordination shell (FCS) of molecules and those outside the FCS<sup>53</sup>.

The traditional bulk liquid-state picture has, in fact, for nonuniform liquids been questioned<sup>55</sup>; in particular, near the confining walls and close to drying transitions. Several promising theories<sup>55–59</sup>, such as Local Molecular Field (LMF) theory<sup>55–58</sup>, have emerged to take into account the importance of the attractive forces in nonuniform liquids. We study here whether the FCS picture (i.e., that interactions beyond the FCS can safely be ignored) of the bulk liquid state holds when considering nanoconfined liquids, in particular, for the wall-liquid interactions. If this turns out to be the case for all liquids or perhaps just for a well-defined class of liquids, a more

---

\*Electronic address: trond@ruc.dk

fundamental or microscopic similarity between bulk and nanoconfined liquids is hereby established.

## II. METHODS

We apply in the current study GPU-optimized *NVT* molecular dynamics computer simulations<sup>60,61</sup> (<http://rumd.org>) of several atomic and molecular model systems in nanoconfinement. The confinement is modelled as a symmetric slit-pore geometry using a smooth external potential<sup>36</sup>. More specifically, the external wall potential is given by

$$v_{9,3}(z) = \frac{4\pi\epsilon_{iw}\rho_w\sigma_{iw}^3}{3} \left[ \frac{1}{15} \left( \frac{\sigma_{iw}}{z} \right)^9 - \frac{1}{2} \left( \frac{\sigma_{iw}}{z} \right)^3 \right]. \quad (1)$$

Here,  $z$  is the distance between the divergence of the potential and the particle in question.  $\sigma_{iw}$  and  $\epsilon_{iw}$  are parameters similar to the Lennard-Jones (LJ) potential, and  $\rho_w$  defines the density of the confining solid. Equation (1) appears after considering the total interaction of a LJ particle with a semi-infinite solid continuum of LJ particles<sup>62</sup> and has been used in some of the earliest studies of confinement<sup>63,64</sup>. Quantities are here and henceforth reported in dimensionless LJ units by setting  $\sigma_{AA} = 1$ ,  $\epsilon_{AA} = 1$ , etc. We use wall-parameters  $\sigma_{Aw} = 1$ ,  $\epsilon_{Aw} = 1$ ; in the case of binary systems  $\sigma_{Bw} = (1 + \sigma_{BB})/2$ ,  $\epsilon_{Bw} = \sqrt{1 \cdot \epsilon_{BB}}$ . The density of the confining solid  $\sigma_w$  is in most cases chosen to be equal to the total average slit-pore density<sup>36</sup>.

However, to perform simulations with FCS cutoffs it has recently been shown<sup>65</sup> that ensuring the continuity of forces is of utmost importance. One method of achieving a continuous force is the so-called shifted-force (SF) cutoff

$$f_{\text{SF}}(r) = \begin{cases} f(r) - f(r_c) & \text{if } r < r_c, \\ 0 & \text{if } r > r_c, \end{cases} \quad (2)$$

which corresponds to adding a linear term  $-v(r_c)(r - r_c) - v(r_c)$  to the original potential  $v(r)$ . In the bulk liquid, these additional terms sum to a good approximation to a constant, and thus do not affect the structure nor the dynamics<sup>53,66</sup>. For the linear term of the liquid-liquid interactions to sum to a constant also near the walls of the confinement, we have found that an additional term beyond the SF-correction on the wall-liquid interactions is needed. We have observed that adding

$$\Delta f = |f_{\text{PAIR}}(r_{ll,\text{FCS}}) - f_{\text{WALL}}(r_{wl,\text{FCS}})|, \quad (3)$$

to the force from the wall (restricted to the FCS) often gives a good cancellation of the linear term near the walls. Here  $r_{ll,\text{FCS}}$  and  $r_{wl,\text{FCS}}$  are, respectively, the distance of the FCS for the liquid-liquid (ll) and wall-liquid

(wl) interactions (see next section for the FCS delimitation) and are thus not free parameters. In the case of different particle-particle interactions we apply cutoffs in units of the largest particle. Applying this particular cutoff method to all FCS simulations, we now present results using FCS cutoffs in nanoconfined liquids.

## III. RESULTS

The investigation is started with Fig. 1 showing the impact of the slit-pore confinement (magenta) on the bulk single-component Lennard-Jones (SCLJ) liquid (blue). Figure 1(a) shows the density profile whereas Fig. 1(b) shows the lateral radial distribution function (RDF). The RDF in the nanoconfinement is calculated for the contact layer (i.e., the layer closest to the walls), and the comparison is performed at the same average density and temperature. The slit-pore has a significant impact on the structure of the liquid showing large density oscillations near the walls, which is also manifested in the RDF obtained near the walls. The contact-layer RDF is quite distinct from the bulk liquid by showing a higher degree of ordering in the liquid. The latter confirms results from other computer simulations of nanoconfined liquids<sup>22,64</sup>.

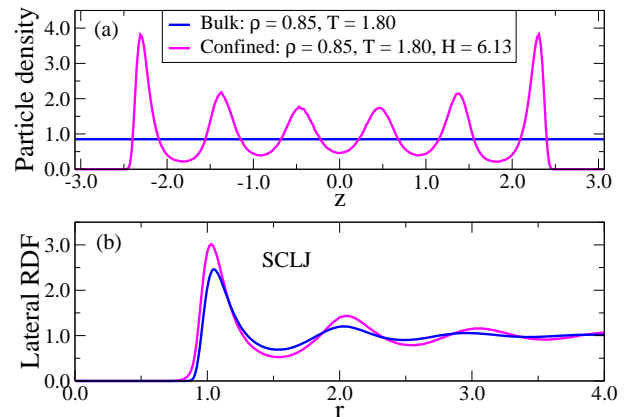


FIG. 1: Impact of the slit-pore confinement (magenta) on the bulk single-component Lennard-Jones (SCLJ) liquid (blue). (a) Density profiles. (b) Lateral RDFs. The RDF in the nanoconfinement is calculated for the contact layer (i.e., the layer closest to the walls) showing a distinct structure from the bulk liquid.

From these observations it appears that the microscopic physics obtained near the walls is actually rather different from the bulk liquid. The latter is also to be expected due to, in general, diverse and complicated wall-liquid interactions.

### A. Simulations of FCS cutoffs

We now proceed to test the bulk FCS picture in nanoconfinement. Figure 2 shows density profiles and contact-layer RDFs for the SCLJ confined state point of Fig. 1. The black curves give a simulation with a large pair potential cutoff in a combination with no cutoff for the wall-liquid interactions. The red dots give results for an FCS cutoff for the liquid-liquid and wall-liquid interactions. The FCSs are delimited<sup>53</sup> via the first minimum of the contact-layer RDF and density profile, respectively. The FCS cutoffs are seen to capture the relevant physics for the entire slit-pore even though the walls modify the structure of liquid quite significantly with respect to the bulk liquid (Fig. 1(b)).

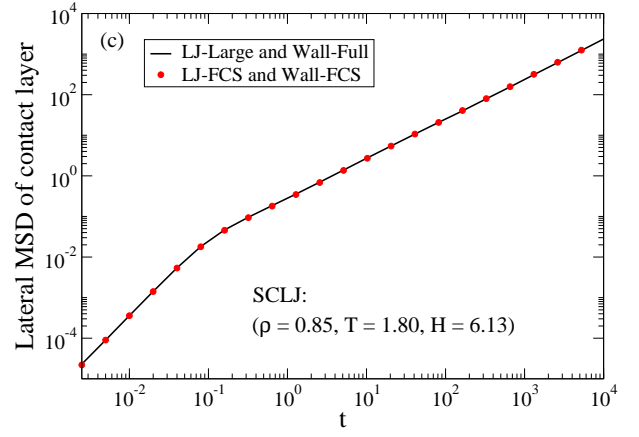
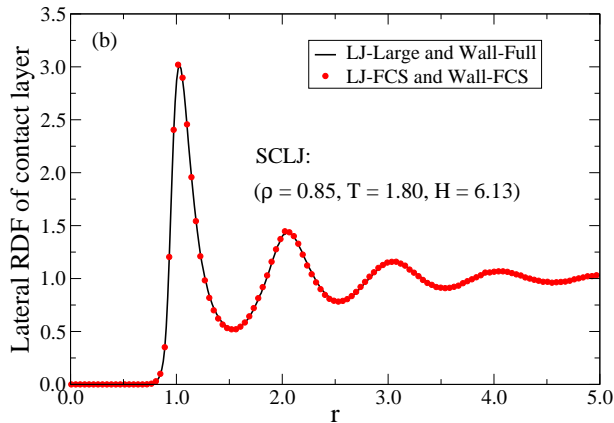
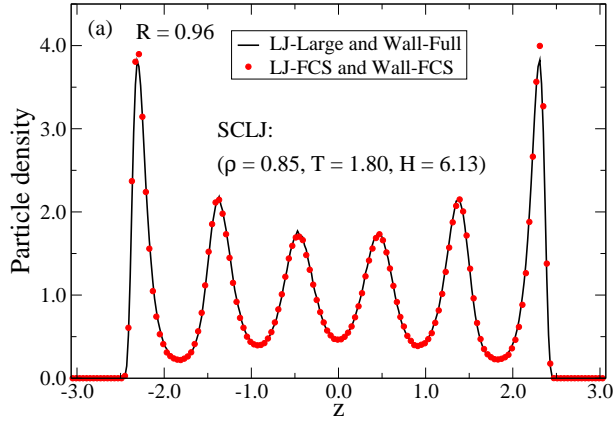
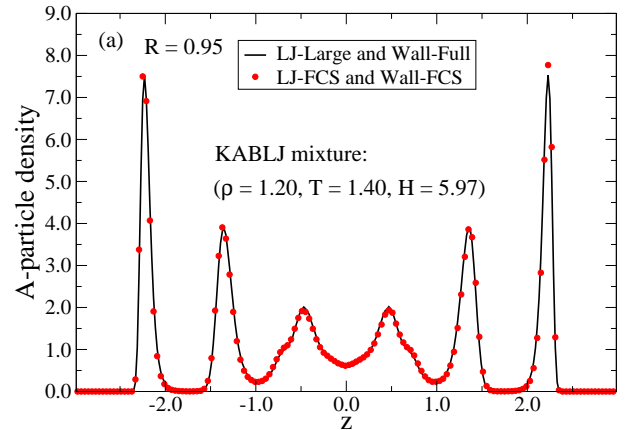


FIG. 2: FCS simulations for the SCLJ liquid in a slit-pore at  $\rho = 0.85$ ,  $T = 1.80$ ,  $H = 6.13$ . The black curves give a simulation with a large pair potential cutoff in a combination with no cutoff for the wall-liquid interactions. The red dots give results for a cutoff at the FCS for the liquid-liquid and wall-liquid interactions ( $r_{ll,FCS} = 1.549$  and  $r_{wl,FCS} = 1.250$ ).  $R$  is the correlation coefficient<sup>67</sup> between  $NVT$  virial and potential energy equilibrium fluctuations and is defined in Eq. (4) below. (a) Density profiles. (b) Lateral RDFs of the contact layer. (c) Lateral mean-square displacements (MSD) of the contact layer.

To test the FCS picture further for nanoconfined liquids, Fig. 3 shows equivalent simulations for the Kob-Andersen binary LJ mixture<sup>68</sup> (KABLJ) at  $\rho = 1.20$ ,  $T = 1.40$ ,  $H = 5.97$ . Figure 3(a) shows  $A$ -particle density profiles, Fig. 3(b) shows lateral RDFs of the contact layer, and Fig. 3(c) shows lateral  $A$ -particle incoherent intermediate scattering functions (ISFs) of the contact layer. The physics near the walls is seen to be captured excellently using the FCS cutoffs.



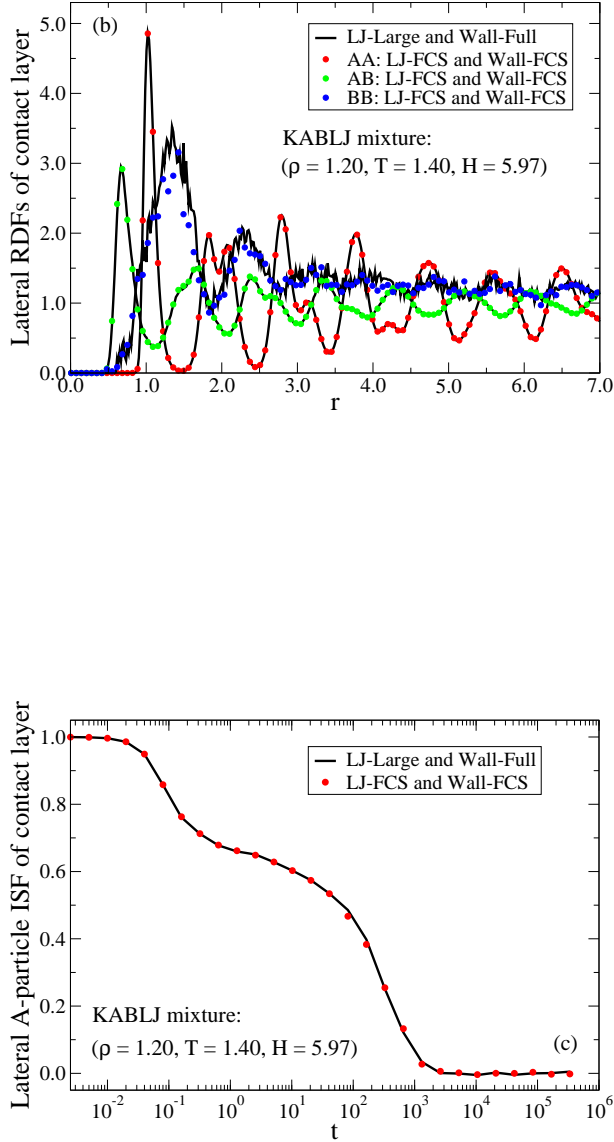


FIG. 3: FCS simulations for the KABLIJ mixture in a slit-pore at  $\rho = 1.20$ ,  $T = 1.40$ ,  $H = 5.97$  ( $r_{ll,FCS} = 1.479$  and  $r_{wl,FCS} = 1.252$ ).  $R$  is defined in Eq. (4). (a) Density profiles. (b) Lateral RDFs of the contact layer. The BB-particle RDF has more noise than the other particle-particle RDFs. (c) Lateral A-particle ISFs of the contact layer.

Proceeding to study in Fig. 4, a small-molecule liquid in terms of the asymmetric dumbbell model<sup>69</sup>, we show lateral contact-layer RDFs and ISFs. Slight deviations are seen with the FCS cutoff for the ISF and are assumed to be attributed to the approximative linear-cancellation term added to the force from the walls.

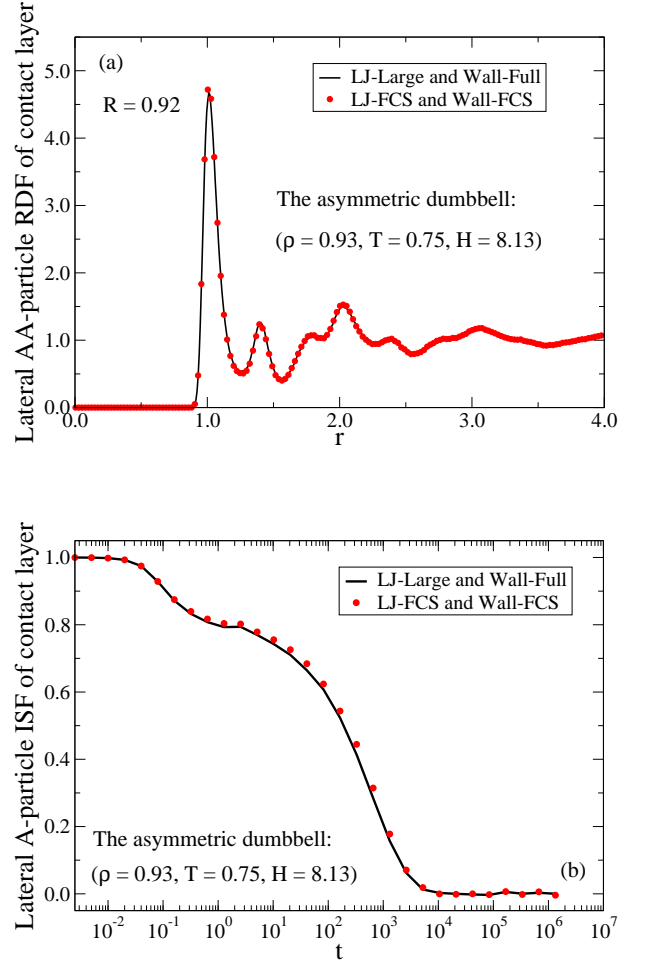


FIG. 4: FCS simulations for the asymmetric dumbbell model in a slit-pore at  $\rho = 0.93$ ,  $T = 0.75$ ,  $H = 8.13$  ( $r_{ll,FCS} = 1.565$  and  $r_{wl,FCS} = 1.015$ ).  $R$  is defined in Eq. (4). (a) Lateral RDFs of the contact layer. (b) Lateral ISFs of the contact layer.

One may wonder how general are these results? The FCS interactions of the bulk liquid were shown in Ref.<sup>53</sup> as the relevant interactions only when the liquid is so-called "Roskilde simple". Roskilde liquids<sup>67</sup> are defined by having the  $NVT$  virial/potential energy correlation coefficient (which depends on the state point),

$$R = \frac{\langle \Delta W \Delta U \rangle}{\sqrt{\langle (\Delta W)^2 \rangle} \sqrt{\langle (\Delta U)^2 \rangle}}, \quad (4)$$

greater than  $R \geq 0.90$ . Only inverse power-law fluids are perfectly correlating ( $R = 1$ ), but many models<sup>53,67</sup> (e.g., the SCLJ liquid, KABLIJ mixture, Lewis-Wahström OTP<sup>70</sup>, and more) as well as some experimental liquids<sup>71,72</sup> have been shown to belong to the class of Roskilde liquids. Roskilde liquids include most or all van der Waals and metallic liquids, whereas covalently, hydrogen-bonding or strongly ionic or dipolar liquids are generally not Roskilde simple<sup>67</sup>. The latter

reflects the fact that directional interactions tend to destroy the strong virial/potential energy correlation.

In all examples studied so far the liquid exhibits strong virial/potential energy correlation in confinement, too ( $R \geq 0.90$ ; see figures). It is possible that as the virial/potential energy correlation decreases, the FCS picture of the nanoconfined liquid becomes a worse approximation. To test this conjecture, we now turn the study to non-Roskilde liquids. One possible way of obtaining a non-Roskilde liquid is to decrease the density for the SCLJ liquid (recall that  $R$  depends on state point). Doing so, we obtain the results of Fig. 5; the correlation coefficient is here  $R = 0.74$ . We observe larger deviations with the FCS cutoff than previously noted and is consistent with the above conjecture.

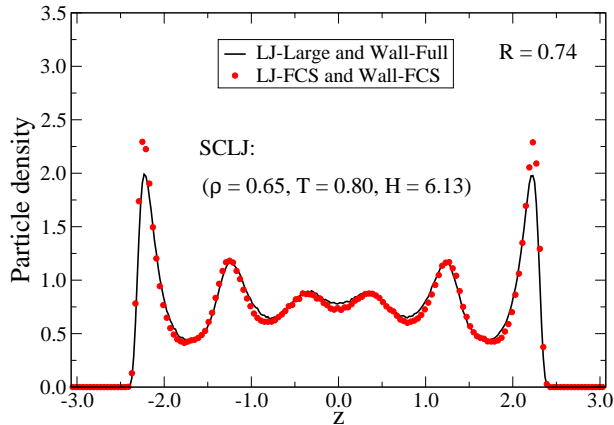


FIG. 5: FCS simulations for the SCLJ liquid in a slit-pore at  $\rho = 0.65$ ,  $T = 0.80$ ,  $H = 6.13$  ( $r_{ll,FCS} = 1.660$  and  $r_{wl,FCS} = 1.377$ ).  $R$  is defined in Eq. (4). At this state point, the SCLJ liquid is not Roskilde simple with  $R = 0.74$ .

As an additional example, we show a simulation in Fig. 6 of the Dzugutov liquid<sup>73</sup> which is also a non-Roskilde liquid with  $R = 0.70$ . Here, the failure of the FCS cutoff in nanoconfinement is rather drastic.

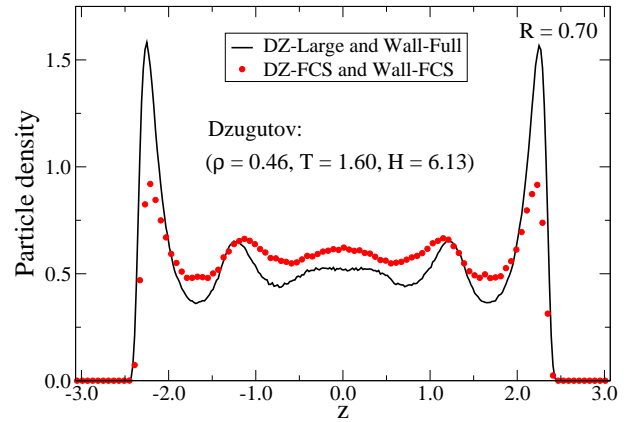
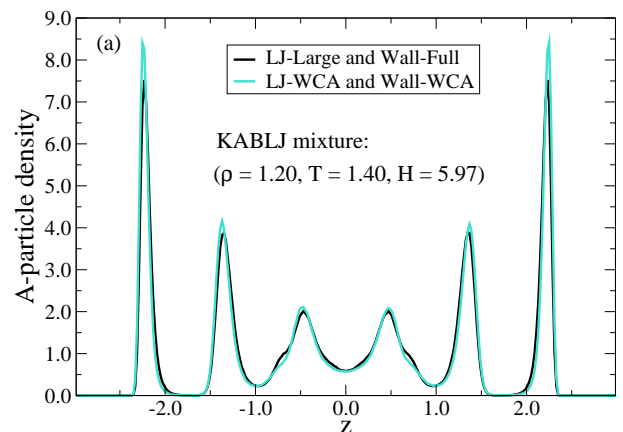


FIG. 6: FCS simulations for the Dzugutov liquid in a slit-pore at  $\rho = 0.46$ ,  $T = 1.60$ ,  $H = 6.13$  ( $r_{ll,FCS} = 1.616$  and  $r_{wl,FCS} = 1.406$ ).  $R$  is defined in Eq. (4). The Dzugutov liquid is not a Roskilde liquid with  $R = 0.70$  at this state point.

## B. Simulations of WCA cutoffs

Having established that for Roskilde liquids it is possible to safely ignore the interactions beyond the FCS for both the liquid-liquid and wall-liquid interactions, we now consider the effect of decreasing the cutoff below the FCS. According to the WCA philosophy in the bulk liquid<sup>51</sup>, it should be possible to cut the potentials at the potential minima and still obtain the correct physics. Applying this method to simulations of confined liquids, we obtain the results of Fig. 7 for the KABLJ mixture. We observe significant discrepancy with the reference simulation hereby confirming results of previous simulations of confined liquids<sup>55,56</sup>.



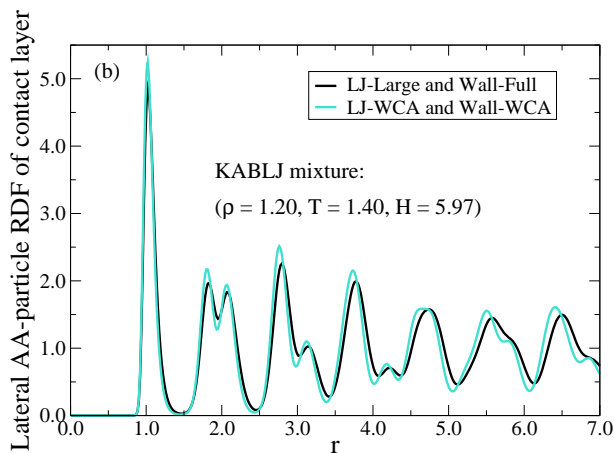


FIG. 7: Simulations of the KABLJ mixture confined to a slit-pore at  $\rho = 1.20$ ,  $T = 1.40$ ,  $H = 5.97$ . The WCA-cutoff method is applied to both the liquid-liquid and wall-liquid interactions. (a)  $A$ -particle density profiles. (b) Lateral AA-particle RDFs of contact layer.

The discrepancy is noted to be the largest near the walls, and to understand this behavior in more detail, we show results in Fig. 8 applying only the WCA approximation on the wall-liquid interactions. Here, no discrepancy is noted.

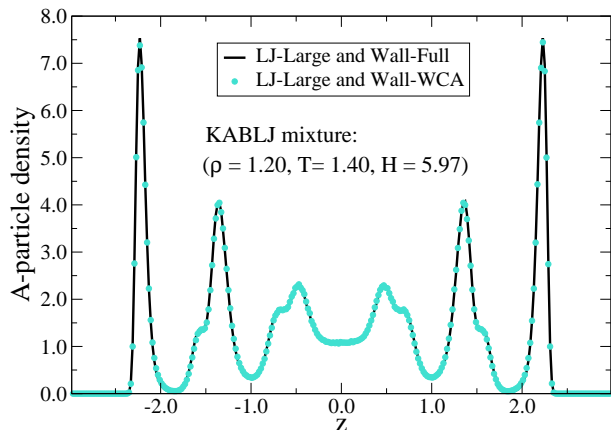


FIG. 8: Simulations of the KABLJ mixture confined to a slit-pore at  $\rho = 1.20$ ,  $T = 1.40$ ,  $H = 5.97$ . The WCA-cutoff method is applied only to the wall-liquid interactions.

From these results one might be tempted to conclude that the FCS is not the fundamental distance for the wall-liquid interactions. The distance of the FCS does, however, depend on density and thus it is possible to perform simulations in which the location of the FCS is pushed far to the left of the potential minimum.

Figure 9 presents results for the confined SCLJ liquid at a very high density state point. The distances of the potential minima are, respectively, for the liquid-liquid and wall-liquid interactions  $2^{1/6}\sigma \approx 1.12$  and

$(2/5)^{1/6}\sigma_w \approx 0.86$ . The FCS cutoffs are, respectively,  $r_{ll,FCS} = 0.934$  and  $r_{wl,FCS} = 0.669$  and thus much smaller than the potential minima. A perfect agreement with the reference simulation is nevertheless obtained confirming that the FCS is indeed the fundamental distance also for the wall-liquid interactions.

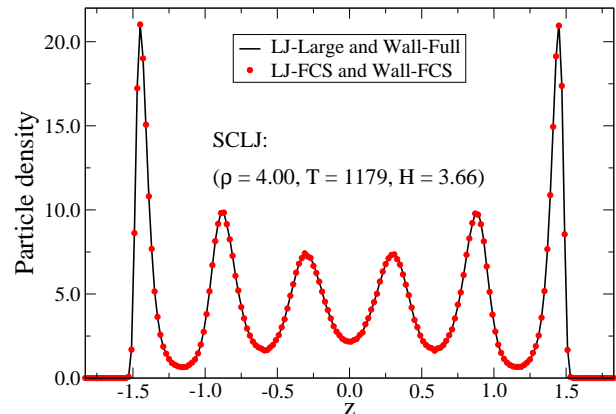


FIG. 9: FCS simulations for the SCLJ liquid in a slit-pore at  $\rho = 4.00$ ,  $T = 1179$ ,  $H = 3.66$ . At this state point the FCSs are pushed to very small distances ( $r_{ll,FCS} = 0.934$  and  $r_{wl,FCS} = 0.669$ ) well below the potential minima ( $2^{1/6}\sigma \approx 1.12$  and  $(2/5)^{1/6}\sigma_w \approx 0.86$ ).

#### IV. CONCLUSION

The results presented here suggest that bulk and nanoconfined liquids are more similar than what is traditionally believed to be the case. The physics as exemplified from the range of interaction is simply as in the bulk liquid; as long as the liquid remains Roskilde simple in confinement. The current study has thus detailed a microscopic similarity between some bulk and nanoconfined liquids in terms of the role of the FCS interactions. It is, however, likely that this observation may also explain the macroscopic similarities between bulk and nanoconfined liquids as they seem to be closely linked to Roskilde liquids<sup>33–36,38</sup>.

Recently, Watanabe *et al.*<sup>22</sup> showed that the dynamics of a confined fluid system as a function of the distance to the walls can be described to a good approximation using the magnitude of the medium-range crystalline order<sup>74</sup> (MRCO). In this perspective, the relevant range of interaction for the wall-liquid interactions is given by the correlation length of MRCO, itself, just as in the bulk liquid. The MRCO perspective is thus fully consistent with the FCS picture proposed here.

We applied in this study an external potential derived from a semi-infinite solid continuum of LJ particles. The SCLJ solid is a Roskilde system<sup>66,67</sup>. Additional studies of more diverse external potentials are thus needed to fully clarify the FCS conjecture proposed here. It is,

however, likely that a requirement of analyticity on the external potential must be placed - similar to the bulk liquid<sup>53</sup>. This is, however, not a crucial restriction since nature is expected to be analytic. In addition, we applied an approximative linear-cancellation term near the walls which worked very well for many systems. We have, however, also encountered state points for the KABLJ mixture where the cancellation was not perfect (not shown). More work in this direction is needed.

The results presented here may provide a foundation for understanding more general interfacial phenomena, which are sensitive to the wall-liquid interactions such as establishment of contact angles on surfaces<sup>75</sup>, interfacial flow<sup>76</sup>, etc. We welcome additional simulation studies of

a wide spectrum of Roskilde liquids/external potentials to further test the FCS picture proposed here.

### Acknowledgments

The center for viscous liquid dynamics "Glass and Time" is sponsored by the Danish National Research Foundation via Grant No. DNRF61. We are grateful to John D. Weeks and Richard Remsing for stimulating correspondence concerning the role of attractive forces in nonuniform liquids.

- 
- [1] B. Bhushan, J. N. Israelachvili and U. Landman, *Nature*, 1995, **374**, 607.
  - [2] G. M. Whitesides, *Nature*, 2006, **442**, 368.
  - [3] J. M. Drake and J. Klafter, *Phys. Today*, 1990, **43**, 46.
  - [4] S. Granick, *Science*, 1991, **253**, 1374.
  - [5] D. Morineau, Y. Xia and C. Alba-Simionesco, *J. Chem. Phys.*, 2002, **117**, 8966.
  - [6] C. L. Jackson and G. B. McKenna, *J. Non-Cryst. Solids*, 1991, **131**, 221.
  - [7] V. Teboul and C. Alba-Simionesco, *Chem. Phys.*, 2005, **317**, 245.
  - [8] M. Alcoutlabi and G. B. McKenna, *J. Phys.: Condens. Matter*, 2005, **17**, 461.
  - [9] B. Coasne, C. Alba-Simionesco, F. Audonnet, G. Dosseh and K. E. Gubbins, *Phys. Chem. Chem. Phys.*, 2011, **13**, 3748.
  - [10] R. Richert, *Annu. Rev. Phys. Chem.*, 2011, **62**, 65.
  - [11] J. L. Keddie, R. A. L. Jones and R. A. Cory, *Europhys. Lett.*, 1994, **27**, 59.
  - [12] A. Serghei, M. Tress and F. Kremer, *Macromolecules*, 2006, **39**, 9385.
  - [13] J. A. Forrest and K. Dalnoki-Veress, *Adv. Colloid Interface Sci.*, 2001, **94**, 167.
  - [14] C. J. Ellison and J. M. Torkelson, *Nat. Mater.*, 2003, **2**, 695.
  - [15] P. Rittigstein, R. D. Priestley, L. J. Broadbelt and J. M. Torkelson, *Nat. Mater.*, 2007, **6**, 278.
  - [16] K. Paeng, R. Richert and M. D. Ediger, *Soft Matter*, 2012, **8**, 819.
  - [17] C. Iacob, J. R. Sangoro, W. K. Kipnusu, R. Valiullin, J. Kärger and F. Kremer, *Soft Matter*, 2012, **8**, 289.
  - [18] Q. Ji, R. Lefort, A. Ghoufi and D. Morineau, *Chem. Phys. Lett.*, 2009, **482**, 234.
  - [19] C. R. Nugent, K. V. Edmond, H. N. Patel and E. R. Weeks, *Phys. Rev. Lett.*, 2007, **99**, 025702.
  - [20] H. B. Eral, D. van den Ende, F. Mugele and M. H. G. Duits, *Phys. Rev. E*, 2009, **80**, 061403.
  - [21] V. N. Michailidou, G. Petekidis, J. W. Swan and J. F. Brady, *Phys. Rev. Lett.*, 2009, **102**, 068302.
  - [22] K. Watanabe, T. Kawasaki and H. Tanaka, *Nat. Mater.*, 2011, **10**, 512.
  - [23] K. V. Edmond, C. R. Nugent and E. R. Weeks, *Phys. Rev. E*, 2012, **85**, 041401.
  - [24] T. Fehr and H. Löwen, *Phys. Rev. E*, 1995, **52**, 4016.
  - [25] J. A. Torres, P. F. Nealey and J. J. de Pablo, *Phys. Rev. Lett.*, 2000, **85**, 3221.
  - [26] P. Scheidler, W. Kob and K. Binder, *J. Phys. IV France*, 2000, **10**, 33.
  - [27] F. W. Starr, T. B. Schröder and S. C. Glotzer, *Macromolecules*, 2002, **35**, 4481.
  - [28] A. R. C. Baljon, M. H. M. V. Weert, R. B. DeGraaff and R. Khare, *Macromolecules*, 2005, **38**, 2391.
  - [29] J. Kurzidim, D. Coslovich and G. Kahl, *Phys. Rev. Lett.*, 2009, **103**, 138303.
  - [30] F. W. Starr and J. F. Douglas, *Phys. Rev. Lett.*, 2011, **106**, 115702.
  - [31] B. A. P. Betancourt, J. F. Douglas and F. W. Starr, *Soft Matter*, 2013, **9**, 241.
  - [32] Y. Rosenfeld, *Phys. Rev. A*, 1977, **15**, 2545.
  - [33] J. Mittal, J. R. Errington and T. M. Truskett, *Phys. Rev. Lett.*, 2006, **96**, 177804.
  - [34] R. Chopra, T. M. Truskett and J. R. Errington, *Phys. Rev. E*, 2010, **82**, 041201.
  - [35] G. Goel, W. P. Krekelberg, M. J. Pond, J. Mittal, V. K. Shen, J. R. Errington and T. M. Truskett, *J. Stat. Mech. Theor. Exp.*, 2009, **4**, 04006.
  - [36] T. S. Ingebrigtsen, J. R. Errington, T. M. Truskett and J. C. Dyre, *Unpublished*, 2013.
  - [37] Y. Rosenfeld and P. Tarazona, *Mol. Phys.*, 1998, **95**, 141.
  - [38] T. S. Ingebrigtsen, A. A. Veldhorst, T. B. Schröder and J. C. Dyre, *Unpublished*, 2013.
  - [39] W. E. Alley and B. J. Alder, *Phys. Rev. A*, 1983, **27**, 3158.
  - [40] K. P. Travis, B. D. Todd and D. J. Evans, *Phys. Rev. E*, 1997, **55**, 4288.
  - [41] J. S. Hansen, P. J. Daivis, K. P. Travis and B. D. Todd, *Phys. Rev. E*, 2007, **76**, 041121.
  - [42] J. S. Hansen, P. J. Daivis, J. C. Dyre, B. D. Todd and H. Bruus, *J. Chem. Phys.*, 2013, **138**, 034503.
  - [43] W. Götze, *Complex Dynamics of Glass-Forming Liquids: A Mode-coupling theory*, Oxford University Press: New York, 1st edn., 2009.
  - [44] V. Krakoviack, *Phys. Rev. Lett.*, 2005, **94**, 065703.
  - [45] G. Biroli, J.-P. Bouchaud, K. Miyazaki and D. R. Reichman, *Phys. Rev. Lett.*, 2006, **97**, 195701.
  - [46] S. Lang, R. Schilling, V. Krakoviack and T. Franosch, *Phys. Rev. E*, 2012, **86**, 021502.
  - [47] D. J. Diestler, M. Schoen, A. W. Hertzner and J. H.

- Cushman, *J. Chem. Phys.*, 1991, **95**, 5432.
- [48] W. P. Krekelberg, V. K. Shen, J. R. Errington and T. M. Truskett, *J. Chem. Phys.*, 2011, **135**, 154502.
  - [49] P. Scheidler, W. Kob and K. Binder, *Europhys. Lett.*, 2000, **52**, 277.
  - [50] B. Widom, *Science*, 1967, **157**, 3787.
  - [51] J. D. Weeks, D. Chandler and H. C. Andersen, *J. Chem. Phys.*, 1971, **54**, 5237.
  - [52] S. Toxvaerd and J. C. Dyre, *J. Chem. Phys.*, 2011, **135**, 134501.
  - [53] T. S. Ingebrigtsen, T. B. Schröder and J. C. Dyre, *Phys. Rev. X*, 2012, **2**, 011011.
  - [54] L. Bøhling, A. A. Veldhorst, T. S. Ingebrigtsen, N. P. Bailey, J. S. Hansen, S. Toxvaerd, T. B. Schröder and J. C. Dyre, *J. Phys.: Condens. Matter*, 2013, **25**, 032101.
  - [55] J. D. Weeks, R. L. B. Selinger and J. Q. Broughton, *Phys. Rev. Lett.*, 1995, **75**, 2694.
  - [56] J. D. Weeks, K. Vollmayr and K. Katsov, *Physica A*, 1997, **244**, 461.
  - [57] J. D. Weeks, K. Katsov and K. Vollmayr, *Phys. Rev. Lett.*, 1998, **81**, 4400.
  - [58] J. M. Rodgers and J. D. Weeks, *J. Phys.: Condens. Matter*, 2008, **20**, 494206.
  - [59] H. Wang, C. Schütte and P. Zhang, *Phys. Rev. E*, 2012, **86**, 026704.
  - [60] S. Toxvaerd, *Mol. Phys.*, 1991, **72**, 159.
  - [61] S. Toxvaerd, O. J. Heilmann, T. Ingebrigtsen, T. B. Schröder and J. C. Dyre, *J. Chem. Phys.*, 2009, **131**, 064102.
  - [62] W. A. Steele, *Surf. Sci.*, 1973, **36**, 317.
  - [63] S. Toxvaerd, *J. Chem. Phys.*, 1981, **74**, 1998.
  - [64] M. Schoen, D. J. Diestler and J. H. Cushman, *J. Chem. Phys.*, 1987, **87**, 5464.
  - [65] S. Toxvaerd and J. C. Dyre, *J. Chem. Phys.*, 2011, **134**, 081102.
  - [66] N. P. Bailey, U. R. Pedersen, N. Gnan, T. B. Schröder and J. C. Dyre, *J. Chem. Phys.*, 2008, **129**, 184508.
  - [67] N. P. Bailey, U. R. Pedersen, N. Gnan, T. B. Schröder and J. C. Dyre, *J. Chem. Phys.*, 2008, **129**, 184507.
  - [68] W. Kob and H. C. Andersen, *Phys. Rev. E*, 1995, **51**, 4626.
  - [69] T. B. Schröder, U. R. Pedersen, N. P. Bailey, S. Toxvaerd and J. C. Dyre, *Phys. Rev. E*, 2009, **80**, 041502.
  - [70] L. J. Lewis and G. Wahnström, *J. Non-Cryst. Solids*, 1994, **172-174**, 69.
  - [71] D. Gundermann, U. R. Pedersen, T. Hecksher, N. P. Bailey, B. Jakobsen, T. Christensen, N. B. Olsen, T. B. Schröder, D. Fragiadakis, R. Casalini, C. M. Roland, J. C. Dyre and K. Niss, *Nat. Phys.*, 2011, **7**, 816.
  - [72] L. A. Roed, D. Gundermann, J. C. Dyre and K. Niss, *arXiv*, 2013, **1**, 1305.4817v2.
  - [73] M. Dzugutov, *Phys. Rev. A*, 1992, **46**, 2984.
  - [74] H. Shintani and H. Tanaka, *Nature*, 2006, **2**, 200.
  - [75] T. Ingebrigtsen and S. Toxvaerd, *J. Phys. Chem. C*, 2007, **111**, 8518.
  - [76] X. Ma, W. Chen, Z. Wang, Y. Peng, Y. Han and P. Tong, *Phys. Rev. Lett.*, 2013, **110**, 078302.